NJC

PAPER

View Article Online
View Journal

Cite this: DOI: 10.1039/c9nj01777a

Ligand-free Cu(II)-catalyzed aerobic etherification of aryl halides with silanes: an experimental and theoretical approach†

Muhammad Naeem Ahmed, *[a] Khalil Ahmad, [b] Khawaja Ansar Yasin,[a]
Tayyaba Farooq,[a] Bilal Ahmad Khan[a] and Soumendra K. Roy *[c]

Owing to their wide occurrence in nature and immense applications in various fields, the synthesis of aryl alkyl ethers has remained a focus of interest. In contrast to the conventional/traditional methods of etherification, herein, we have reported a more efficient method, which is better yielding and more general in application. The etherification of aryl halides by alkoxy/phenoxy silanes was catalyzed by copper acetate in the presence of cesium carbonate and oxygen in DMF at 145 °C. All the as-synthesized compounds were characterized *via* the ^{1}H-NMR and ^{13}C-NMR spectroscopic techniques. Density functional theory calculations using the B3LYP functional were performed to elucidate the reaction mechanism. The C–O coupling reaction between 2-nitroiodobenzene and tetramethoxysilane was used as a model reaction. The activation energy barriers for the generation of catalytic species (31.6 kcal mol^{-1}) and the σ-bond metathesis (16.0 kcal mol^{-1}), oxidative addition/reductive elimination (20.3 kcal mol^{-1}), halogen atom transfer (19.2 kcal mol^{-1}) and single electron transfer (SET) (29.5 kcal mol^{-1}) mechanisms for the C–O coupling reaction were calculated. Calculations for the key reaction steps were repeated with the B3PW91, PBEH1PBE, wB97XD, CAM-B3LYP and mPW1LYP functionals. The formation of catalytic species *via* a single electron transfer reaction between tetramethoxysilane and copper acetate, formation of methoxy radicals and methoxylation of copper showed an overall energy barrier of 31.6 kcal mol^{-1}, and therefore is the rate determining step.

Received 7th April 2019,
Accepted 17th June 2019

DOI: 10.1039/c9nj01777a

rsc.li/njc

1. Introduction

The prime interest in the field of organic synthesis is the selective formation of the carbon–oxygen bond at a specific position of an arene since the aryl ether functionality is abundantly found in agrochemicals, pharmaceuticals, materials science, polymers and natural products.[1–5] There are numerous examples of aryl ether-containing compounds in pharmaceuticals such as esomeprazole,[6] pioglitazone[7] and venlafaxine.[8]

The classical methods to synthesize aryl ethers include Williamson ether synthesis *via* aromatic nucleophilic substitution of aryl halides with phenoxides and Ullmann coupling of haloarenes with phenols. Both reactions require harsh reaction conditions and show limited substrate scope, making them inappropriate for the functionalization of multifaceted organic molecules at the advanced stage of a synthetic series.[9] Thus, extensive research has been conducted for the development of new methods for the selective synthesis of ether linkages that can be used for the late-stage functionalization of complex organic molecules in a complex synthetic sequence.[10–13]

Contemporary methods involve transition metal-catalyzed sp^2 C–O bond formation by two main groups. Palladium-[14–16] and copper-catalyzed[17–19] Buchwald–Hartwig-type coupling takes place between electrophilic aryl halides with nucleophilic phenols and alcohols.[20–24] Palladium catalysts are limited to phenols and alcohols with no β-hydrogen atom, whereas aliphatic alcohols bearing a β-hydrogen atom require a more complex ligand system to attain good yields of the aryl/alkyl ethers under palladium catalysis. Copper complexes and salts are generally used to synthesize aryl ethers from aryl halides and alcohols since they do not promote β-hydride elimination. Copper-aided oxidative etherification of aryl nucleophiles produced from aryl boronic acids[25–29] and arenecarboxylic acid-based nucleophiles[30] represent the second category to

---

[a] Department of Chemistry, The University of Azad Jammu & Kashmir, Muzaffarabad 13100, Pakistan. E-mail: drnaeem@ajku.edu.pk
[b] Department of Chemistry, Mirpur University of Science and Technology (MUST), Mirpur 10250 (AJK), Pakistan
[c] Institute of Theoretical and Computational Chemistry, Shaanxi Key Laboratory of Catalysis, School of Chemical & Environmental Science, Shaanxi University of Technology, Hanzhong, Shaanxi 723001, P. R. China. E-mail: soumya029@yahoo.in

† Electronic supplementary information (ESI) available. See DOI: 10.1039/c9nj01777a

access aryl ethers. In both reactions, a stoichiometric quantity of copper acetate is used in the presence of an oxidant. The former Chan–Evan–Lam coupling of aryl boronic acids is limited to the synthesis of biaryl ethers, whereas the latter decarboxylative approach produces only aryl alkyl ethers by using alkoxy silanes, while phenoxylation is executed by using triphenoxyborane.

For copper-assisted etherification, the use of alkoxy silanes is an attractive approach due to the wide availability of alkoxylated and aryloxylated silanes either synthetically[31] or commercially. With the development of new approaches that involve the synthesis of both alkyl aryl ethers and aryl aryl ethers, the use of silicon-based etherification reagents will be valued by the synthetic chemical community. We hypothesized that the use of silanes with aryl halides instead of arenecarboxylic acids as etherification reagents can extend the scope to diaryl ethers as well as aryl alkyl ethers.

The kinetics and thermodynamics of the copper-catalyzed C–N and C–O cross coupling reactions between aryl halides and *N*- and *O*-nucleophiles have been studied widely by experimentalists[32–37] as well as theorists.[38–45] Theoretical studies/investigations have focused on oxidative addition/reductive elimination, σ-bond metathesis, single electron transfer (SET) and halogen atom transfer mechanisms. The density functional theory (DFT) studies by Jones *et al.*[38] favoured the single electron transfer mechanism for the β-diketone promoted *N*-arylation of methylamine and halogen atom transfer mechanism for the 1,10-phenanthroline-promoted *O*-arylation of methanol, disfavouring the oxidative addition/reductive elimination and σ-bond metathesis mechanisms. However, subsequent theoretical studies by Yu *et al.* indicated the oxidative addition/reductive elimination mechanism for the β-diketone-promoted *N*-arylation and the 1,10-phenanthroline-promoted *O*-arylation of amino alcohols.[40] Several other theoretical studies on copper-catalyzed C–N and C–O coupling reactions have supported the oxidative addition/reductive elimination mechanism.[40–45]

In the present study, we established an efficient method for the synthesis of diaryl and aryl alkyl ethers *via* the coupling reaction of aryl halides with alkoxy and aryloxy silanes in the presence of copper acetate. We also explored the oxidative addition/reductive elimination, σ-bond metathesis, single electron transfer and halogen atom transfer mechanisms for this reaction. These theoretical studies will help to understand the reaction mechanism and hence in the further improvement of catalytic systems.

2. Experimental

All catalytic reactions were performed in oven-dried 20 mL glass vials equipped with a Teflon-coated stirring bar and a septum cap at ambient oxygen pressure. Aryl halides and different silanes were purchased from J&K Scientific Limited China. *tert*-Butyldimethyl(phenoxy)silanes were prepared according to the reported procedure.[46,47] Copper catalysts were provided by Alfa Aesar, while other reagents were supplied by Acros and Merck. The progress of the reactions was monitored by thin-layer chromatography and purification was achieved through flash column chromatography (FCC). ^{1}H-NMR (400 MHz) and ^{13}C-NMR (100 MHz) spectra were recorded on a JEOL JNM-ECA instrument in $CDCl_3$, while J values were calculated in Hz. Melting points were determined using a Yanaco melting point apparatus and reported as uncorrected.

2.1 General procedure for the synthesis of alkyl aryl ethers and biaryl ethers

A mixture of aryl halide (1.0 mmol), silane (1.5 mmol) and copper acetate (20 mol%) in 4 mL of DMF was stirred at 145 °C for 18 h under ambient oxygen pressure. After cooling to room temperature, the reaction mixture was diluted with 30 mL of dichloromethane. The resultant mixture was washed with water (2 × 30 mL), brine (30 mL), and dried over anhydrous magnesium sulfate. The solvent was removed under vacuum and the residue was purified by flash column chromatography (petroleum ether: ethyl acetate) to obtain the corresponding ethers (**2a–2z**).

1-Methoxy-2-nitrobenzene (2a)

Yellow liquid, yield = 85%, ^{1}H-NMR (400 MHz, $CDCl_3$) δ ppm 7.84 (m, 1H), 7.56–7.54 (m, 1H), 7.08–7.02 (m, 2H), 3.95 (s, 3H); ^{13}C-NMR δ ppm 152.8, 139.6, 134.1, 125.5, 120.2, 113.4, 56.3.

1-Ethoxy-2-nitrobenzene (2b)

Yellow liquid, yield = 81%, ^{1}H-NMR (400 MHz, $CDCl_3$) δ ppm 7.99 (m, 1H), 7.50 (m, 1H), 7.08–6.99 (m, 2H), 4.18 (q, 2H, J = 6.9 Hz), 1.45 (t, 3H, J = 6.9 Hz); ^{13}C-NMR δ ppm 152.1, 139.8, 133.9, 125.2, 119.9, 114.3, 65.1, 14.3.

1-*n*-Propoxy-2-nitrobenzene (2c)

Yellow liquid, yield = 77%, ^{1}H-NMR (400 MHz, $CDCl_3$) δ ppm 7.72 (dd, 1H, J_1 = 7.8 Hz, J_2 = 1.8 Hz), 7.44–7.41 (m, 1H), 6.99 (m, 1H), 6.91 (m, 1H), 3.97 (t, 2H, J = 6.4 Hz), 1.78 (s, 2H, J = 6.4 Hz), 0.98 (t, 3H, J = 7.8 Hz); ^{13}C-NMR δ ppm 152.2, 139.8, 133.9, 125.3, 119.9, 114.3, 70.9, 22.3, 10.34.

1-*n*-Butoxy-2-nitrobenzene (2d)

Yellow liquid, yield = 80%, ^{1}H-NMR (400 MHz, $CDCl_3$) δ ppm 7.81 (m, 1H), 7.49 (m, 1H), 7.0 (m, 2H), 4.10 (t, 2H, J = 6.4 Hz), 1.81 (q, 2H, J = 5.9 Hz), 1.51 (s, 2H, J = 7.3 Hz), 0.97 (t, 3H, J = 7.6 Hz).^{13}C-NMR δ ppm 152.4, 140.0, 133.9, 125.4, 119.9, 114.3, 69.2, 30.9, 19.0, 13.7.

Methyl 2-methoxybenzoate (2e)

Colorless liquid, yield = 86%, ^{1}H-NMR (400 MHz, $CDCl_3$) δ ppm 7.79 (m, 1H), 7.44 (m, 1H), 6.98–6.94 (m, 2H), 3.88 (s, 3H), 3.87 (s, 3H); ^{13}C-NMR δ ppm 166.5, 158.9, 133.3, 131.4, 119.8, 111.8, 55.7, 51.8.

Ethyl 2-ethoxybenzoate (2f)

Colorless liquid, yield = 81%, ^{1}H-NMR (400 MHz, $CDCl_3$) δ ppm 7.77 (m, 1H), 7.43 (m, 1H), 6.96 (m, 2H), 4.34 (q, 2H, J = 7.3 Hz), 4.10 (q, 2H, *J* = 7.3 Hz), 1.44 (t, 3H, *J* = 7.3 Hz), 1.37 (t, 3H, *J* = 7.3 Hz); ^{13}C-NMR δ ppm 166.4, 158.3, 133.0, 131.3, 120.8, 119.9, 113.1, 64.4, 60.6, 14.6, 14.4.

Ethyl 4-ethoxybenzoate (2g)

Colorless liquid, yield = 79%, ^{1}H-NMR (400 MHz, $CDCl_3$) δ ppm 7.98 (d, 2H, *J* = 5.4 Hz), 6.88 (d, 2H, *J* = 5.4 Hz), 4.34 (q, 2H, *J* = 7.3 Hz), 4.08 (q, 2H, *J* = 6.9 Hz), 1.42 (t, 3H, *J* = 7.3 Hz), 1.37 (t, 3H, *J* = 6.9 Hz); ^{13}C-NMR δ ppm 166.3, 162.6, 131.4, 122.7, 113.9, 63.6, 14.6, 14.0.

Methyl 2-*n*-propoxybenzoate (2h)

Colorless liquid, yield = 75%, ^{1}H-NMR (400 MHz, $CDCl_3$) δ ppm 7.78–7.46 (m, 2H), 6.96–6.93 (m, 2H), 3.99 (t, 2H, *J* = 6.4 Hz), 3.88 (s, 3H), 1.84 (s, 2H, *J* = 7.3 Hz), 1.06 (t, 3H, *J* = 7.8 Hz); ^{13}C-NMR δ ppm 166.9, 158.5, 133.2, 131.4, 120.3, 119.9, 113.1, 70.3, 51.8, 22.5, 10.4.

Methyl 2-*n*-butoxybenzoate (2i)

Colorless liquid, yield = 70%, ^{1}H-NMR (400 MHz, $CDCl_3$) δ ppm 7.77–7.41 (m, 2H), 6.95–6.93 (m, 2H), 4.02 (t, 2H, *J* = 6.4 Hz), 3.87 (s, 3H), 1.80 (s, 2H, *J* = 5.9 Hz), 1.53 (q, 2H, *J* = 7.3 Hz), 0.97 (t, 3H, *J* = 7.3 Hz); ^{13}C-NMR δ ppm 166.8, 158.5, 133.1, 131.4, 120.3, 119.8, 112.9, 68.4, 51.7, 31.1, 19.0, 13.6.

2-Methoxybenzaldehyde (2j)

Light yellow solid, m.p. = 36–38 °C, yield = 60%, ^{1}H-NMR (400 MHz, $CDCl_3$) δ ppm 10.4 (s, 1H), 7.84 (m, 1H), 7.55 (m, 1H), 7.0 (m, 2H), 3.93 (s, 3H); ^{13}C-NMR δ ppm 189.7, 181.8, 135.8, 128.5, 124.8, 120.6, 111.6, 55.6.

1-Methoxy-2-(trifluoromethyl)benzene (2k)

Colorless liquid, yield = 51%, ^{1}H-NMR (400 MHz, $CDCl_3$) δ ppm 7.57 (m, 2H), 7.01 (m, 2H), 3.90 (s, 3H); ^{13}C-NMR δ ppm 157.7 (q, J_{C-F} = 1.9 Hz), 133.2, 127.0 (q, J_{C-F} = 5.6 Hz), 125.0 (q, J_{C-F} = 272.8 Hz), 119.9, 111.9 (q, J_{C-F} = 31.4 Hz), 55.8.

2-Methoxybenzaldehyde (2l)

Colorless liquid, yield = 86%, ^{1}H-NMR (400 MHz, $CDCl_3$) δ ppm 7.79 (m, 1H), 7.44 (m, 1H), 6.98–6.94 (m, 2H), 3.88 (s, 3H), 3.87 (s, 3H); ^{13}C-NMR δ ppm 166.5, 158.9, 133.3, 131.4, 119.8, 111.8, 55.7, 51.8.

Methyl 3-methoxybenzoate (2m)

Colorless liquid, yield = 56%, ^{1}H-NMR (400 MHz, $CDCl_3$) δ ppm 7.62 (m, 1H), 7.56 (m, 1H), 7.35 (m, 1H), 7.10 (m, 1H), 3.91 (s, 3H), 3.85 (s, 3H); ^{13}C-NMR δ ppm 166.8, 159.4, 131.3, 129.2, 121.8, 119.3, 113.8, 55.3, 52.0.

Methyl 4-methoxybenzoate (2n)

White solid, m.p. = 46–48 °C, yield = 80%, ^{1}H-NMR (400 MHz, $CDCl_3$) δ ppm 7.98 (d, 2H, *J* = 6.9 Hz), 6.91 (d, 2H, *J* = 6.9 Hz), 3.88 (s, 3H), 3.85 (s, 3H); ^{13}C-NMR δ ppm 166.8, 163.2, 131.5, 122.5, 113.5, 55.3, 51.7.

1-Methoxy-4-nitrobenzene (2o)

White solid, m.p. = 51–53 °C, yield = 80%, ^{1}H-NMR (400 MHz, $CDCl_3$) δ ppm 8.23 (d, 2H, *J* = 7.3 Hz), 6.99 (d, 2H, *J* = 7.3 Hz), 3.94 (s, 3H); ^{13}C-NMR δ ppm 164.5, 141.4, 125.8, 113.9, 55.9.

1-Phenoxy-2-nitrobenzene (2p)

Pale yellow liquid, yield = 82%, ^{1}H-NMR (400 MHz, $CDCl_3$) δ ppm 7.95–7.38 (m, 4H), 7.18–7.03 (m, 5H); ^{13}C-NMR δ ppm 155.7, 150.7, 141.3, 134.0, 130.0, 125.6, 124.5, 123.0, 120.4, 119.2.

Methyl 2-phenoxybenzoate (2q)

Colorless liquid, yield = 75%, ^{1}H-NMR (400 MHz, $CDCl_3$) δ ppm 7.91–7.41 (m, 2H), 7.30–6.94 (m, 7H), 3.78 (s, 3H); ^{13}C-NMR δ ppm 166.0, 157.5, 156.0, 133.4, 131.7, 129.6, 123.3, 123.0, 120.7, 118.0, 52.0.

Methyl 4-phenoxybenzoate (2r)

White solid, m.p. = 57–59 °C, yield = 77%, ^{1}H-NMR (400 MHz, $CDCl_3$) δ ppm 8.00 (d, 2H, *J* = 6.9 Hz), 7.40–7.16 (m, 3H), 7.05 (d, 2H, *J* = 6.4 Hz), 6.99 (d, 2H, *J* = 8.7 Hz), 3.80 (s, 3H); ^{13}C-NMR δ ppm 166.6, 161.7, 155.6, 131.6, 130.0, 124.4, 120.0, 117.2, 51.9.

1-(3-Methoxyphenoxy)-2-nitrobenzene (2s)

Pale yellow liquid, yield = 77%, ^{1}H-NMR (400 MHz, $CDCl_3$) δ ppm 7.94–7.25 (m, 4H), 7.06–6.61 (m, 4H), 3.78 (s, 3H); ^{13}C-NMR δ ppm 161.1, 156.8, 150.4, 141.3, 134.0, 130.4, 125.6, 123.2, 120.7, 111.0, 110.2, 105.2, 55.4.

Methyl 4-(4-methoxyphenoxy)benzoate (2t)

White solid, m.p. 99–101 °C, yield = 71%, ^{1}H-NMR (400 MHz, $CDCl_3$) δ ppm 7.99 (d, 2H, *J* = 6.9 Hz), 7.00 (d, 2H, *J* = 6.4 Hz), 6.93–6.90 (m, 4H), 3.88 (s, 3H), 3.82 (s, 3H); ^{13}C-NMR δ ppm 166.6, 162.7, 156.6, 148.6, 131.5, 123.8, 121.6, 116.2, 115.0, 55.6, 51.9.

Methyl 4-(4-nitrophenoxy)benzoate (2u)

Solid, m.p. 108–110 °C, yield = 74%, ^{1}H-NMR (400 MHz, $CDCl_3$) δ ppm 8.26 (d, 2H, *J* = 9.1 Hz), 8.11 (d, 2H, *J* = 9.1 Hz), 7.26–7.08 (m, 4H), 3.93 (s, 3H); ^{13}C-NMR δ ppm 166.1, 161.8, 158.9, 143.4, 132.0, 126.8, 119.4, 118.3, 52.2.

Methyl-4-(4-(*tert*-butyl)phenoxy)benzoate (2v)

Colorless liquid, yield = 69%, ^{1}H-NMR (400 MHz, $CDCl_3$) δ ppm 7.99 (d, 2H, *J* = 6.8 Hz), 7.39 (d, 2H, *J* = 6.8 Hz), 6.99–6.96 (m, 4H), 3.88 (s, 3H), 1.33 (s, 9H); ^{13}C-NMR δ ppm 166.6, 162.1, 153.0, 147.4, 131.5, 126.7, 124.1, 119.5, 117.0, 51.9, 34.4, 31.4.

Methyl 4-(*p*-tolyloxy)benzoate (2w)

White solid, m.p. 60–62 °C, yield = 73%, ^{1}H-NMR (400 MHz, $CDCl_3$), δ ppm 8.00–7.46 (m, 2H), 7.25–7.16 (m, 2H), 7.01–6.93 (m, 4H), 3.88 (s, 3H), 2.35 (s, 3H); ^{13}C-NMR δ ppm 166.6, 162.2, 153.1, 134.2, 131.5, 130.4, 124.0, 120.1, 116.8, 51.9, 20.7.

Methyl 4-(3-methoxyphenoxy)benzoate (2x)

Colorless liquid, yield = 68%, ^{1}H-NMR (400 MHz, $CDCl_3$) δ ppm 7.99 (d, 2H, J = 6.9 Hz), 7.25 (t, 1H, J = 8.2 Hz), 6.99 (d, 2H, J = 6.9 Hz), 7.00–6.61 (m, 3H), 3.88 (s, 3H), 3.76 (s, 3H); ^{13}C-NMR δ ppm 166.6, 161.5, 156.6,131.5, 130.3, 124.4, 117.3, 111.9, 110.0, 105.9, 55.2, 51.8.

Methyl 4-(2-methoxyphenoxy)benzoate (2y)

Colorless liquid, yield = 70%, ^{1}H-NMR (400 MHz, $CDCl_3$) δ ppm 7.96 (d, 2H, J = 6.8 Hz), 7.30–6.98 (m, 6H), 3.87 (s, 3H), 3.78 (s, 3H); ^{13}C-NMR δ ppm 166.6, 162.2, 151.6, 143.3, 131.4, 126.0, 123.8, 122.2, 121.2, 115.7, 112.9, 55.8, 51.8.

Methyl 2-(3-methoxyphenoxy)benzoate (2z)

Colorless liquid, yield = 69%, ^{1}H-NMR (400 MHz, $CDCl_3$) δ ppm 7.91–7.46 (m, 2H), 7.20–7.00 (m, 2H), 6.56–6.50 (m, 4H), 3.80 (s, 3H), 3.75 (s, 3H); ^{13}C-NMR δ ppm 166.0, 160.8, 158.7, 155.8, 133.4, 131.7, 130.0, 123.5, 123.1, 120.9, 110.1, 108.6, 104.1, 55.2, 55.0.

3. Results and discussion

For the synthesis of alkyl aryl ethers and diaryl ethers using silanes as etherification reagents, we started our investigations with the highly reactive 2-nitroiodobenzene and tetramethoxysilane in DMF at 145 °C. After 18 h, 2-nitroiodobenzene was fully recovered even in the absence and presence of a base, indicating that the aromatic nucleophilic substitution mechanism was absent (entries 1 and 2). When the reaction was conducted in the presence of 20 mol% of copper acetate, 2-nitroiodobenzene was converted into the 2-nitroanisole in 45% yield, indicating the role of the copper catalyst (entry 3). The presence of oxygen dramatically increased the yield to 84%, confirming the mechanistic proposition of Stahl[48] (entry 4). The screening of different quantities of copper sources and bases showed that 20 mol% of the copper acetate catalyst provided the optimum yield in the presence of 2 equivalents of cesium carbonate (entries 5–16). Testing of various ligands and oxidants resulted in a decrease in the yield of the reaction. The solvent screening showed that the polar aprotic DMF is the solvent of choice for the etherification reaction. The temperature and time optimization showed that the reaction is best performed at 145 °C for 18 h, and lower than that resulted a decrease in the yield (Table 1).

Table 1 Optimization of the reaction conditions[a]

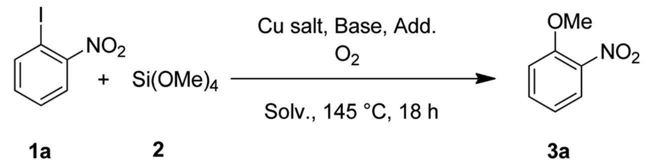

#	Catalyst	Base	Additive	Solvent	Yield
1	—	—	—	DMF	—
2	—	Cs_2CO_3	—	DMF	—
3	$Cu(OAc)_2$	Cs_2CO_3	—	DMF	45
4	$Cu(OAc)_2$	Cs_2CO_3	O_2	DMF	84
5	$CuF_2\cdot 2H_2O$	Cs_2CO_3	O_2	DMF	30
6	$CuSO_4$	Cs_2CO_3	O_2	DMF	Trace
7	Cu(II)formate·$4H_2O$	Cs_2CO_3	O_2	DMF	20
8	$Cu(OBz)_2\cdot 2H_2O$	Cs_2CO_3	O_2	DMF	56
9	$Cu_3(PO)_4$	Cs_2CO_3	O_2	DMF	Trace
10	$Cu(OAc)_2$	Cs_2CO_3	O_2	DMF	25[b]
11	$Cu(OAc)_2$	Cs_2CO_3	O_2	DMF	17[c]
12	$Cu(OAc)_2$	Cs_2CO_3	O_2	DMF	40[d]
13	$Cu(OAc)_2$	Cs_2CO_3	O_2	DMF	50[e]
14	$Cu(OAc)_2$	NaOH	O_2	DMF	—
15	$Cu(OAc)_2$	K_2CO_3	O_2	DMF	49
16	$Cu(OAc)_2$	Ag_2CO_3	O_2	DMF	Trace
17	$Cu(OAc)_2$	Ag_2O	O_2	DMF	Trace
18	$Cu(OAc)_2$	$(C_2H_5)_3N$	O_2	DMF	41
19	$Cu(OAc)_2$	Cs_2CO_3	O_2	DMSO	60
20	$Cu(OAc)_2$	Cs_2CO_3	O_2	NMP	47
21	$Cu(OAc)_2$	Cs_2CO_3	O_2	Toluene[f]	—
22	$Cu(OAc)_2$	Cs_2CO_3	O_2	Acetonitrile[g]	—
23	$Cu(OAc)_2$	Cs_2CO_3	BQ	DMF	—
24	$Cu(OAc)_2$	Cs_2CO_3	1,10-Phenan.	DMF	10
25	$Cu(OAc)_2$	Cs_2CO_3	PPh_3	DMF	33

[a] Reaction conditions: 2-nitroiodobenzene (1 mmol), $Si(OMe)_4$ (1.5 mmol), Cat. (20 mol%), Cs_2CO_3 (2 eq.), 4 mL Solv., 145 °C, 18 h. Isolated yields. [b] $Cu(OAc)_2$ (15 and 10 mol% respectively). [c] $Cu(OAc)_2$ (15 and 10 mol% respectively). [d] 100 °C. [e] 12 h. [f] 105 °C and 95 °C. [g] 105 °C and 95 °C.

Having established the optimized reaction protocol for the methoxylation of 2-nitroiodobenzene with tetramethoxysilane in the presence of 20 mol% of copper acetate and ambient oxygen pressure at 145 °C for 18 h, we next tested the scope of the transformation with regard to the *O*-nucleophile and aryl halides (Table 2).

Among the *O*-nucleophiles tested, methoxy, ethoxy, *n*-propoxy and *n*-butoxy groups were smoothly transferred from silanes to aromatic rings (**2a–d**). In addition to alkoxy groups, phenoxy and substituted phenoxy groups were also transferred from silane to the substituted iodobenzenes to produce the respective diaryl ethers in good yields (**2p–z**). In earlier reports, boron reagents were employed to access diaryl ethers.[30] The reaction conditions are tolerant to various substituents including ether, nitro and *tert*-butyl on the phenyl ring of the *O*-nucleophiles.

After successful transfer of alkoxy and phenoxy groups from silane partner, we next investigated the scope of the transformation with respect to aryl halides. The results showed that the reaction methodology is not restricted to aryl iodides (**2e–2j**), and aryl bromides and even aryl chlorides produced above 40% of the corresponding ethers (**2l**, **2n**, **2t**, **2x**, **2y**, **2z** and **2a**). In case of aryl bromides and chlorides, the presence of an electron withdrawing group is necessary, whereas aryl iodides produce aryl ethers even in the absence of electron withdrawing groups.

4. Mechanistic studies

4.1 Computational details

DFT calculations were performed using the Gaussian09 suite of programs[49] using the unrestricted UB3LYP functional.[50–52] All geometries were optimized using the 6-31G(d) basis set for H, C, N and O atoms. Copper atom was described with the Stuttgart RSC 1997 ECP basis set with 10 core electrons. For the iodine atom, the LANL2DZ effective core potential of Hay

Table 2 Scope of the transformation

Entry	Aryl halides	Silanes	Product	Yields (%)
1	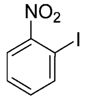 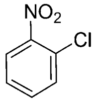	$Si(OMe)_4$	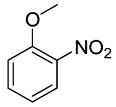 **2a**	85 40
2	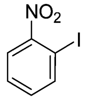	$Si(OEt)_4$	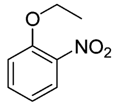 **2b**	81
3	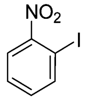	$Si(OPr)_4$	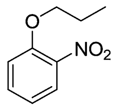 **2c**	77
4	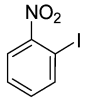	$Si(OBu)_4$	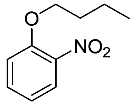 **2d**	80
5	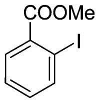	$Si(OMe)_3Me$	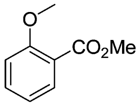 **2e**	86
6	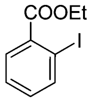	$Si(OEt)_4$	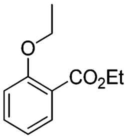 **2f**	81
7	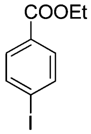	$Si(OEt)_4$	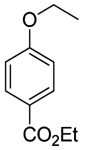 **2g**	79
8	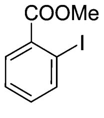	$Si(OPr)_4$	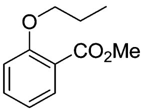 **2h**	75
9	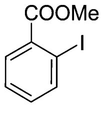	$Si(OBu)_4$	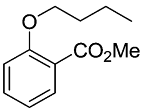 **2i**	70
10	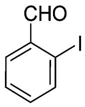	$Si(OMe)_4$	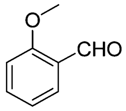 **2j**	60

Table 2 (*continued*)

Entry	Aryl halides	Silanes	Product	Yields (%)
11	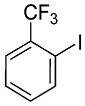	$Si(OMe)_4$	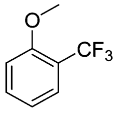 **2k**	51
12	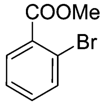	$Si(OMe)(CH_3)_3$	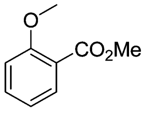 **2l**	86
13	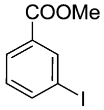	$Si(OMe)_4$	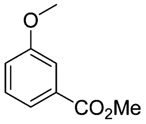 **2m**	56
14	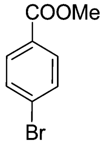	$Si(OMe)_4$	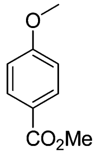 **2n**	80
15	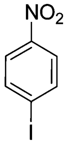	$Si(OMe)_4$	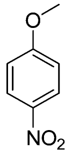 **2o**	80
16	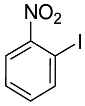	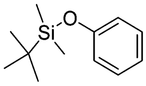	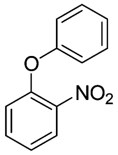 **2p**	82
17	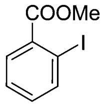	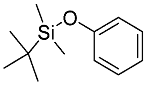	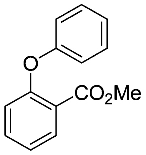 **2q**	75
18	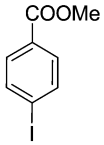	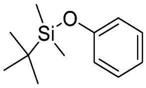	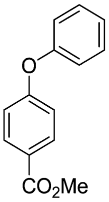 **2r**	77
19	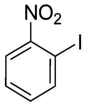	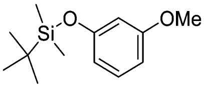	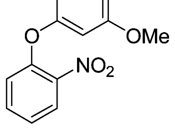 **2s**	77

Table 2 (*continued*)

Entry	Aryl halides	Silanes	Product	Yields (%)
20	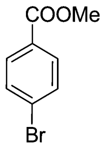	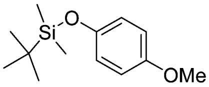	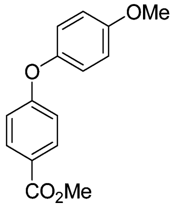 **2t**	71
21	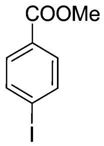	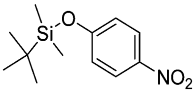	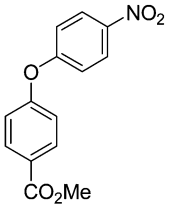 **2u**	74
22	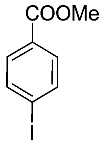	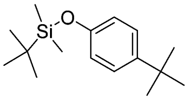	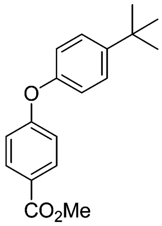 **2v**	69
23	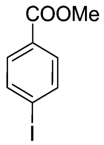	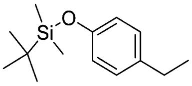	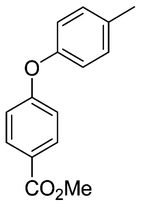 **2w**	73
24	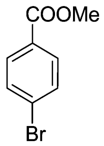	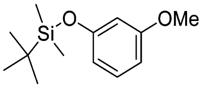	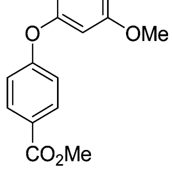 **2x**	68
25	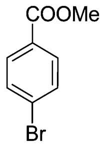	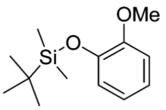	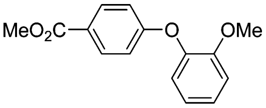 **2y**	68
26	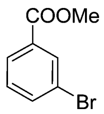	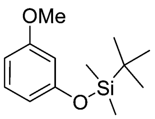	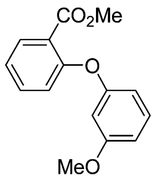 **2z**	69

and Wadt augmented with additional p and d polarization functions (exponents 0.0308 and 0.2940, respectively) was used.[53] The Berny algorithm was used to optimize the transition states.[54] All ground and transition states were verified by vibrational frequency analysis. Intrinsic reaction coordinate calculations were performed to confirm the transition states. The CPCM solvent model was employed to consider the solvent effects.[55–57] Single point energy calculations in the solution phase were erformed with the unrestricted UB3LYP, UB3PW91, UPBEH1PBE, UwB97XD, UCAM-B3LYP and UmPW1LYP functionals using the 6-311+G(d,p) basis set for H, C, N and O atoms. For copper and iodine atoms, the cc-pVTZ-PP basis sets were used. The solvent parameters for DMF solvent ($\varepsilon = 36.71$) are not available in Gaussian09; therefore, the solvent parameters for acetonitrile ($\varepsilon = 36.64$) were employed. A similar approach has been adopted elsewhere in the literature.[38]

4.2 Generation of the catalytic species

Copper-catalyzed C–N and C–O cross-coupling reactions are catalyzed by the three common oxidation states of copper, *i.e.* Cu(0), Cu(I) and Cu(II).[58–72] The Cu(I)-catalyzed reactions are slightly faster than Cu(0) and Cu(II). It is believed that Cu(I) is the actual catalyst for these reactions and both Cu(0) and Cu(II) are converted to Cu(I) prior to the initiation of the catalytic reactions.[73–78] Experimental studies also support the conversion of Cu(0) and Cu(II) to Cu(I) in their catalytic reactions.[79–88] For CuH-based catalytic systems, the catalytically active Cu(I) species ''LCuH'' is formed by the reaction of Cu(II) acetate with a stoichiometric amount of trialkoxyhydrosilanes ($(RO)_3SiH$).[89–92] In our reaction, tetramethoxysilane is used instead of trialkoxyhydrosilane, and we propose that tetramethoxysilane reacts with copper(II) acetate to give LCu^1OMe species, where L can be a methoxy (**Int1**; $[Cu(OCH_3)_2]^-$), acetate group (**Int2**; $[Cu(OCH_3)(CH_3COO)]^-$) or a DMF molecule (**Int3**; $[Cu(OCH_3)(DMF)]$).

The optimized geometries and relative energies of **Int1**, **Int2** and **Int3** are given in Fig. 1. Among the three plausible intermediates, intermediate **Int1** is 16.8 and 27.6 kcal more stable than intermediates **Int2** and **Int3**, respectively.

The mechanistic studies performed by Selvakumar *et al.* for the copper-mediated etherification of heteroarenes with alkoxysilanes supported the radical mechanism for the reaction.[93] The transfer of single electron from alkoxysilanes to copper(II) acetate affords alkoxysilane radicals, which undergo Si–O bond cleavage to deliver the alkoxy radicals. In the reaction system under investigation, the tetramethoxysilane could undergo radical reaction by transferring a single electron to copper(II) acetate. The Gibbs free energy of the electron transfer reaction was calculated from the energies of the separated reactants and products of the reaction.[38] The activation energy for the electron transfer was calculated from the Gibbs free energy of the reaction using the Marcus–Hush model.[94–101] The calculated activation energy barrier for the electron transfer reaction between tetramethoxysilane and copper(II) acetate is 105.7 kcal mol^{-1} (Scheme 1). Due to the very high activation energy barrier, the transfer of electrons from tetramethoxysilane to copper(II) acetate was ruled out.

It has been observed that in the presence of anions, the tetra-coordinated silicon compounds form penta- and hexa-coordinated species.[102] Hence, the carbonate anion could react with the tetramethoxysilane to give tetramethoxysilicon carbonate, which could undergo single electron transfer reaction, and the Gibbs free energy for the formation of tetramethoxysilicon carbonate is +2.3 kcal mol^{-1}. The single electron transfer (SET) reaction of tetramethoxysilicon carbonate and further reaction steps describing the formation of methoxy radicals, methoxylation of copper by the methoxy radicals and activation of methoxysilane compounds by electron transfer reactions with Cu(II) are represented by reactions (a) to (h) in Scheme 2.

In reaction step (a), a single electron is transferred from tetramethoxysilicon carbonate to copper(II) acetate, and the calculated Gibbs free energy and the activation energy barrier for the single electron transfer reaction are 4.4 and 6.8 kcal mol^{-1}, respectively. In reaction step (b), the tetramethoxysilicon carbonate radical (compound **3**) disintegrates to produce trimethoxysilicon carbonate (compound **5**) and a methoxy radical *via* the transition state $TS_{(b)}$. In step (c), the methoxy radical displaces an acetate ligand from complex **4** to yield Cu(II) complex **6.** In step (d), an acetate group adds to compound **5** to produce compound **7**, the formation of the compound **7** is endothermic by 12.2 kcal mol^{-1}. In step (e), the compound **7** transfers single electron to the Cu(II) complex **6** to afford a radical compound **8** and Cu(I) complex **9**, and the Gibbs free energy and activation energy for the single electron transfer reaction are 8.4 and 9.8 kcal mol^{-1}, respectively. In step (f), the radical compound **8** disintegrates to provide a methoxy radical *via* the transition state $TS_{(f)}$, and the activation energy of $TS_{(f)}$ is 15.5 kcal mol^{-1}. In reaction step (g), the methoxy radical created

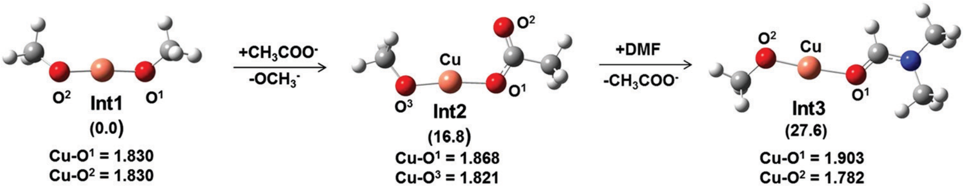

Fig. 1 Optimized geometries of **Int1**, **Int2** and **Int3** (values within parentheses represent relative Gibbs free energies in kcal mol^{-1}).

$$Si(OCH_3)_4 + Cu(OAc)_2 \longrightarrow [Si(OCH_3)_4]^{\cdot} + [Cu(OAc)_2]^- \quad \Delta G_r = 69.8\ \text{kcal/mol}, \quad E_a = 105.7\ \text{kcal/mol}$$

Scheme 1 Gibbs free energy and activation energy barrier for the single electron transfer reaction between tetramethoxysilane and copper(II) acetate.

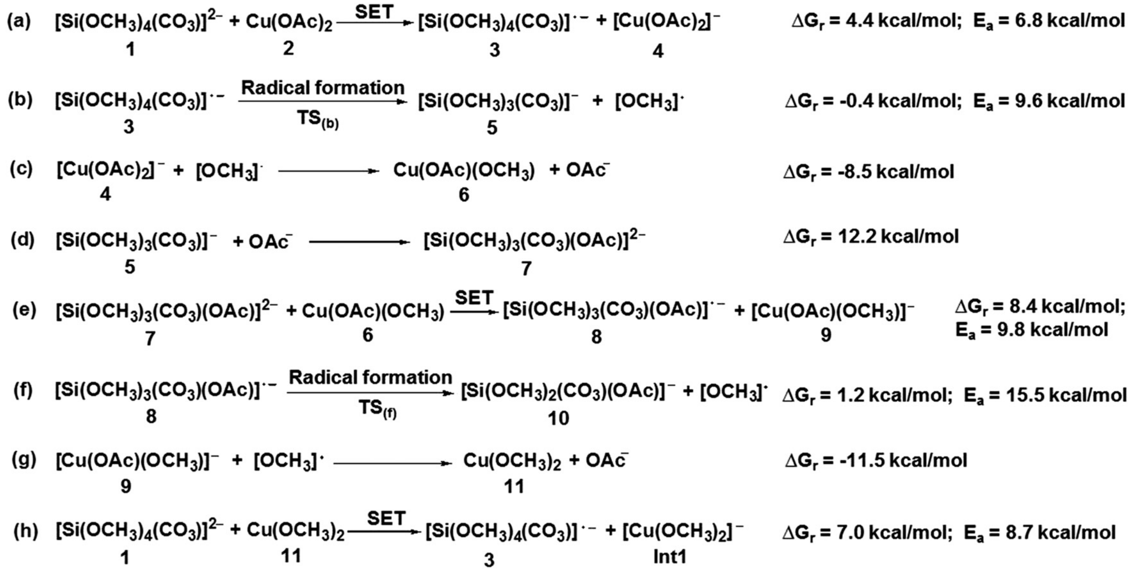

Scheme 2 Calculated Gibbs free energies for reaction steps (a–h) and activation energies for steps (a), (b), (e), (f) and (h).

in step (f) reacts with Cu(I) complex **9** to afford Cu(II) complex **11**. In step (h), the tetramethoxysilicon carbonate reduces the Cu(II) complex **11** to Cu(I) complex (**Int1**). The overall reaction comprises three single electron transfer reactions, whereas each tetramethoxysilicon carbonate provides two electrons, and thus the use of 1.5 equivalents of tetramethoxysilane in the reaction is justified.

The energy level diagram depicting the Gibbs free energies of reaction steps (a) to (h), activation energies of steps (a), (b), (e), (f) and (h), and the overall activation energy barrier is presented in Fig. 2. The overall barrier for reactions (a) to (h) is 31.6 kcal mol^{-1}.

4.3 Activation of C–I bond of aryl iodide and C–O coupling reaction

Four mechanisms, *i.e.* oxidative addition/reductive elimination (OA/RE), σ-bond metathesis, single electron transfer (SET) and halogen atom transfer (HAT) reaction, were studied for the mechanistic investigations of copper-catalyzed C–N and C–O cross coupling reactions between aryl halides and *N*- and *O*-nucleophiles.[38–45] A general scheme representing the methoxylation of 2-nitroiodobenzene with tetramethoxysilane *via* different mechanisms is depicted in Scheme 3.

In the oxidative addition/reductive elimination mechanism, the aryl halide adds to the Cu(I) complex to yield a Cu(III)

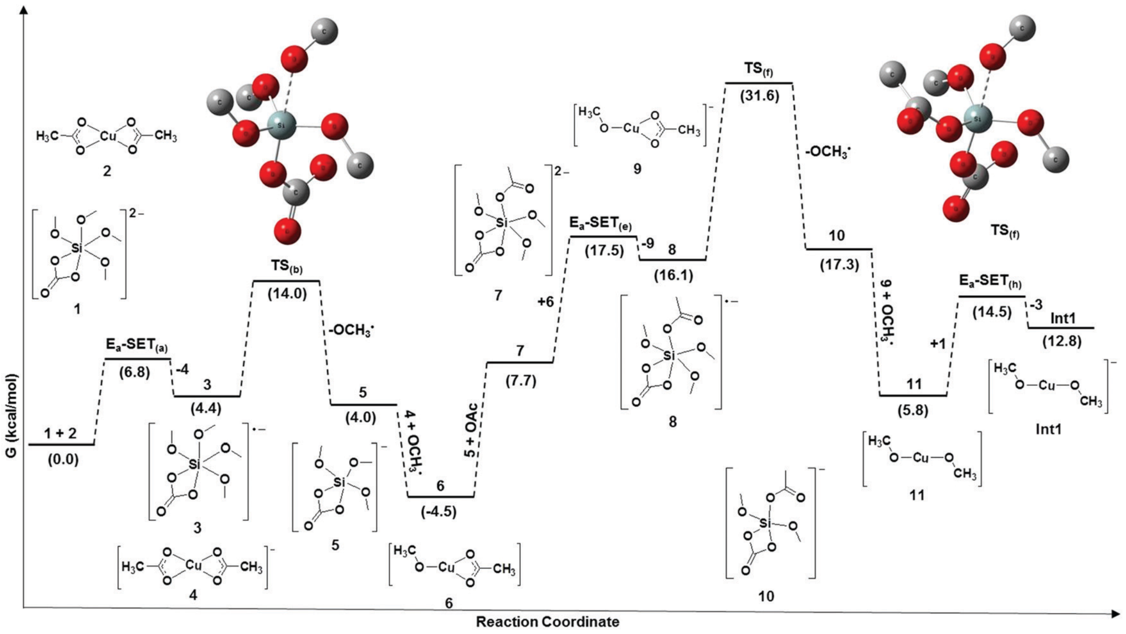

Fig. 2 Energy level diagram for the generation of catalytic species through reaction steps (a) to (h).

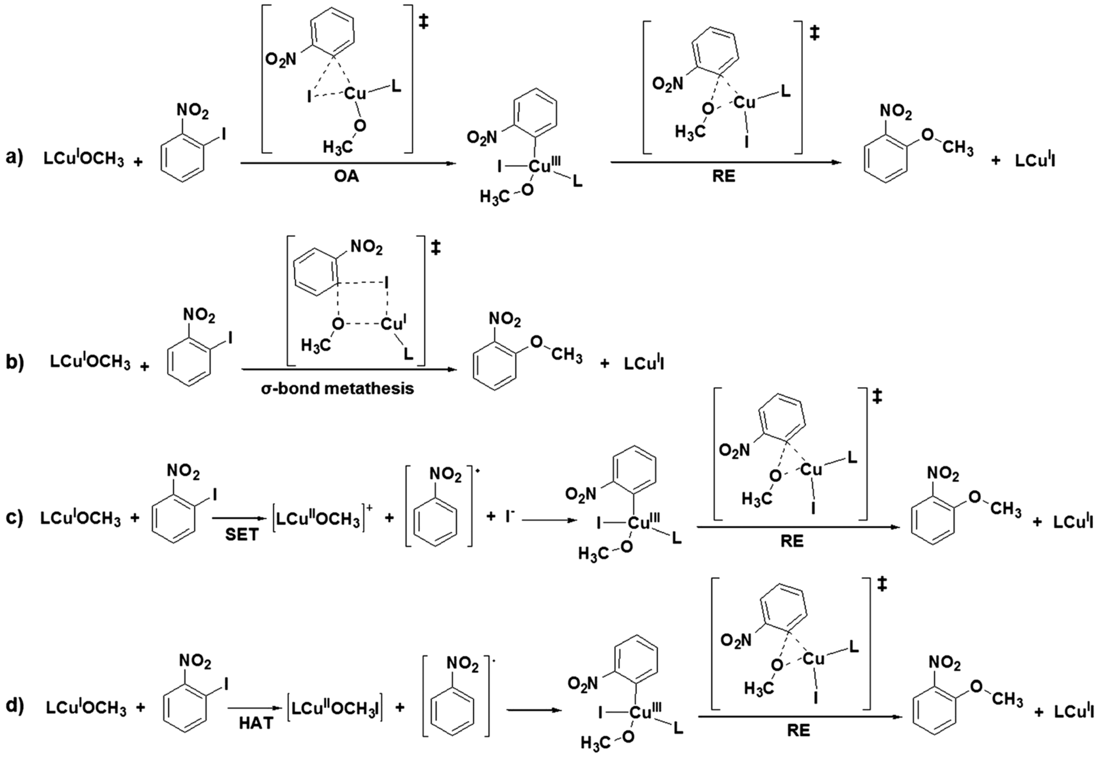

Scheme 3 General scheme representing: (a) oxidative addition/reductive elimination (OA/RE), (b) σ-bond metathesis, (c) single electron transfer (SET) and (d) halogen atom transfer (HAT) mechanisms for the methoxylation of 2-nitroiodobenzene with tetramethoxysilane.

intermediate. The Cu(III) intermediate undergoes reductive elimination to produce the coupling product and Cu(I) species, which is available for another catalytic cycle. The energy level diagram for the oxidative addition/reductive elimination reactions of **Int1** and **Int2** is displayed in Fig. 3. The intermediate **Int1** undergoes oxidative addition reaction with 2-nitroiodobenzene *via* a three-centered transition state **Int1-TS$_{OA}$** to yield the Cu(III) intermediate **Int1-M1**. The calculated activation energy for the oxidative addition step is 20.3 kcal mol^{-1} and the free energy for the formation of **Int1-M1** is −7.2 kcal mol^{-1}. The intermediate **Int1-M1** undergoes reductive elimination to yield 1-methoxy-2-nitrobenzene and a Cu(I) species (**Int1-M2**). The activation energy for the reductive elimination reaction is 10.0 kcal mol^{-1} and the free energy for the overall reaction is −43.7 kcal mol^{-1}. In the overall reaction, the oxidative addition is the rate-limiting step with an activation energy of 20.3 kcal mol^{-1}. For **Int2**, the activation energy for the oxidative addition and reductive elimination steps is 22.5 and 3.7 kcal mol^{-1}, respectively. The overall barrier for the oxidative addition/reductive elimination mechanism of **Int2** is 39.3 kcal mol^{-1}.

The optimized geometries of the transition states and the different reaction intermediates are presented in Fig. 4.

In the σ-bond metathesis mechanism, the copper atom remains in the 1+ oxidation state throughout the catalytic cycle. The aryl halide bond is activated *via* a four-centered transition state between the aryl halide and the copper catalyst. The energy level diagram for the activation of the C–I bond of aryl iodide by σ-bond metathesis reaction of **Int1** and **Int2** is presented in Fig. 5. The calculated activation energies for the σ-bond metathesis reaction of **Int1** and **Int2** are 16.0 and 16.5 kcal mol^{-1} and the overall barriers are 16.0 and 33.3 kcal mol^{-1}, respectively.

Copper complexes **Int1** and **Int2** can transfer a single electron to aryl iodide to activate the C–I bond. The transfer of the electron can take place either in a stepwise or a concerted manner. In the stepwise electron transfer, the activation energy was estimated using the outer-sphere Marcus–Hush model.[94–101] In the concerted method, the activation energy was estimated using Savéant's model,[103–105] which includes the effect of C–I bond cleavage energy in the estimation of activation energy. The Gibbs free energy of the single electron transfer reactions was calculated from the energies of the separated reactants and products of the reaction.[38] The Gibbs free energies for the outer- and inner-sphere single electron transfer reactions of **Int1** and **Int2** are presented in Scheme 4.

In the halogen atom transfer mechanism, the iodine atom of the aryl halide is transferred to the Cu(I) complex. The transition state for the iodine atom transfer could not be located after many attempts. Therefore, the activation energy for the iodine atom transfer was taken to be equal to the free energy of the iodine atom transfer reaction, and a similar approach has been adopted in the literature.[38,106] The Gibbs free energies for the iodine atom transfer reaction of **Int1** and **Int2** are described in Scheme 5.

The calculated activation energy barriers for the single electron transfer and halogen atom transfer mechanisms of **Int1** and **Int2** are given in Table 3.

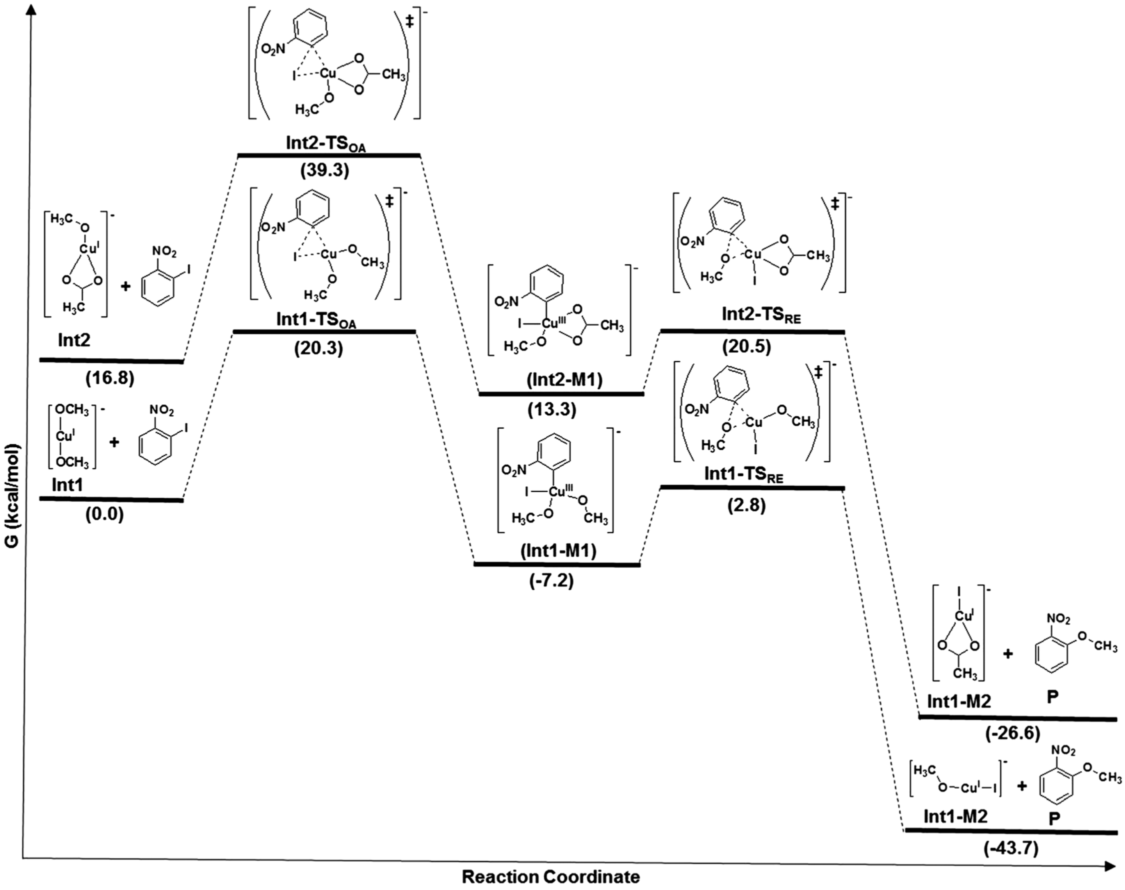

Fig. 3 Energy profile for the oxidative addition/reductive elimination mechanism of **Int1** and **Int2** (values in parentheses represent the Gibbs free energy in kcal mol^{-1}).

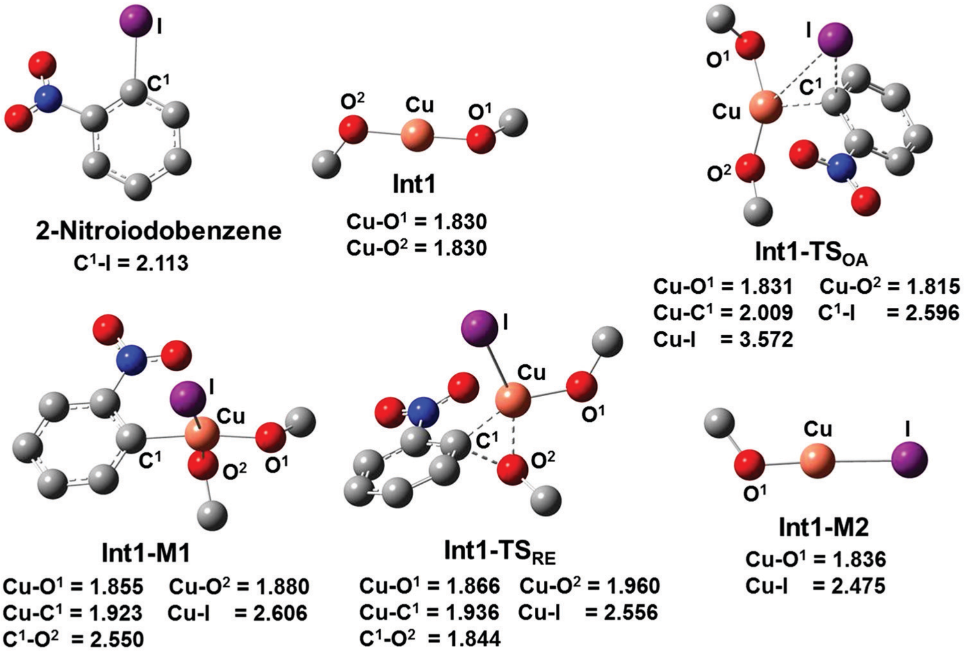

Fig. 4 Optimized geometries of the different species in the oxidative addition/reductive elimination reaction of **Int1** (H atoms are removed for clarity and bond lengths are given in Å).

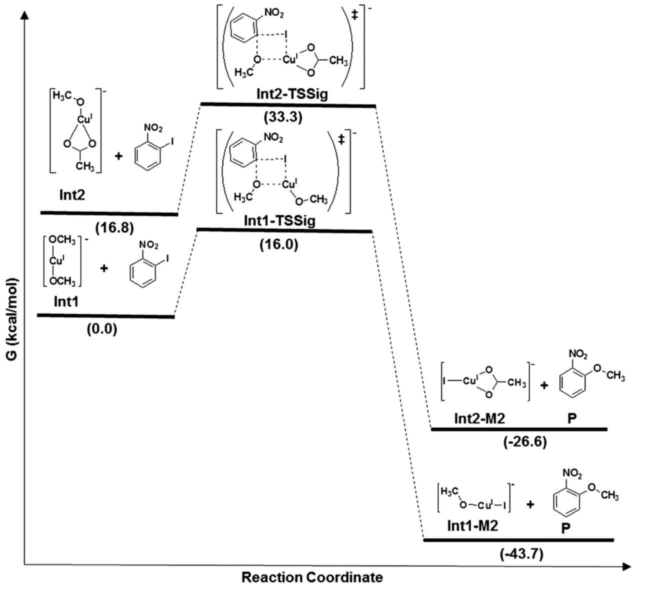

Fig. 5 Energy profile for the σ-bond metathesis mechanism of **Int1** and **Int2** (values in parentheses represent the Gibbs free energy in kcal mol^{-1}).

The activation energy barrier for the activation of the C–I bond of 2-nitroiodobenzene is lower for intermediate **Int1** than **Int2** for all four mechanisms investigated theoretically, and the σ-bond metathesis mechanism showed the lowest activation energy. Interestingly, this is in contrast to the copper-catalyzed C–N coupling reactions, which proceeded mainly *via* the oxidative addition/reductive elimination mechanism.[39–45] The computed activation energy for the σ-bond metathesis mechanism is very low under the given reaction conditions (145 °C, 18 h). Further investigations were carried out by calculating the key reaction steps of the σ-bond metathesis, oxidative addition/reductive elimination and iodine atom transfer mechanism of **Int1** with the B3PW91, PBEH1PBE, wB97XD, CAM-B3LYP and mPW1LYP functionals, including a DMF molecule in the coordination sphere of copper, and by calculating the activation energy barriers for iodobenzene and comparing them with that of 2-nitroiodobenzene (Table 4).

With all the DFT functionals used, the σ-bond metathesis mechanism displayed the lowest barrier for the activation of the C–I bond of 2-nitroiodobenzene. Moreover, the oxidative addition reaction showed the lowest barrier for the activation of iodobenzene, which is much higher than that for 2-nitroiodobenzene, and furthermore the inclusion of a DMF molecule in the coordination sphere of copper changed the activation energies. For further insight into the reaction mechanism, the Gibbs free energies for the dissociation of the C–I bond of 2-nitroiodobenzene and iodobenzene were calculated. The calculated Gibbs free energy for the dissociation of the C–I

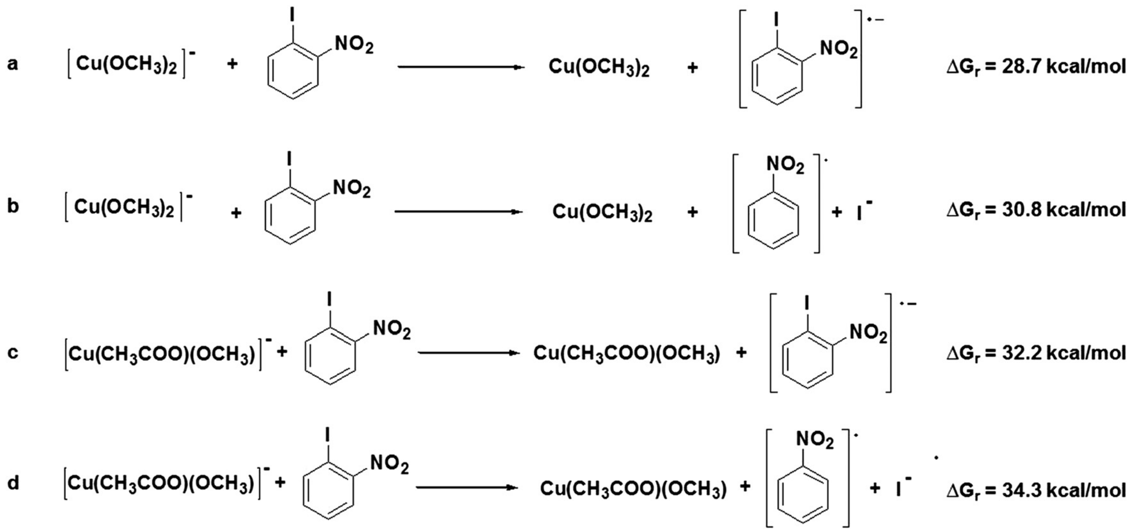

Scheme 4 Gibbs free energy for the outer-sphere (a and c) and inner-sphere (b and d) single electron transfer reactions of **Int1** and **Int2**.

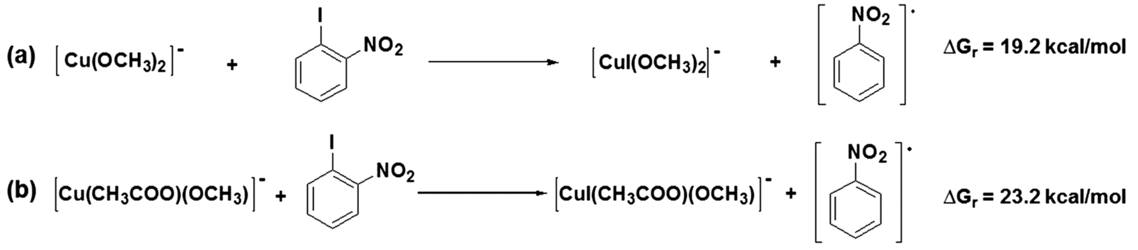

Scheme 5 Gibbs free energies for the iodine atom transfer reaction of **Int1** and **Int2**.

Table 3 Gibbs free energies (ΔG_r), activation energies (E_a) and overall barriers for single electron transfer (SET) and halogen atom transfer mechanisms of **Int1** and **Int2**

Intermediate	Mechanism	ΔG_r (kcal mol^{-1})	E_a (kcal mol^{-1})	Overall barrier (kcal mol^{-1})
Int1	Outer sphere SET[a]	28.7	29.5	29.5
Int1	Inner sphere SET[b]	30.8	35.9	35.9
Int1	Halogen atom transfer	19.2	19.2	19.2
Int2	Outer sphere SET[a]	32.2	35.0	51.8
Int2	Inner sphere SET[b]	34.3	38.6	55.4
Int2	Halogen atom transfer	23.2	23.2	23.2

[a] Stepwise electron transfer (Marcus–Hush model). [b] Concerted electron transfer (Savéant's model).

Table 4 The C–I bond activation energies of 2-nitroiodobenzene and iodobenzene calculated with different DFT functionals and by adding a DMF molecule to the coordination sphere of Cu

	Activation energy (kcal mol^{-1})					
	2-Nitroiodobenzene			Iodobenzene		
DFT functional	σ-Bond metathesis	OA	IAT	σ-Bond metathesis	OA	IAT
B3LYP	16.0	20.3	19.2	26.8	24.2	24.4
B3PW91	14.4	19.2	19.3	25.6	22.7	24.2
PBEH1PBE	11.6	18.3	18.6	23.1	21.3	23.4
wB97XD	10.7	23.1	23.2	23.3	23.7	27.8
CAM-B3LYP	16.1	28.2	21.0	28.0	29.0	25.9
mPW1LYP	15.4	21.4	17.2	26.5	24.8	22.4
B3LYP[a]	16.6	20.6	19.2	—	—	—

[a] Activation energies calculated by adding DMF molecule to the coordination sphere of Cu.

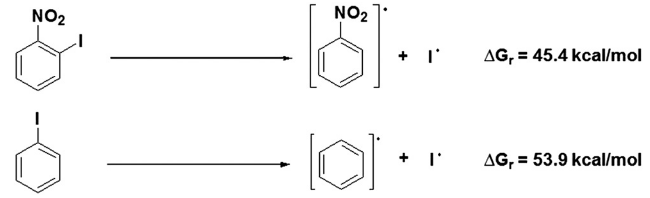

Scheme 6 Gibbs free energy for the dissociation of the C–I bond of 2-nitroiodobenzene and iodobenzene.

bond of 2-nitroiodobenzene (8.5 kcal mol^{-1}) is significantly lower than the C–I bond dissociation energy of iodobenzene (Scheme 6). The lower C–I bond dissociation energy of 2-nitroiodobenzene is plausibly responsible for its very facile cleavage through the σ-bond metathesis reaction.

4.4 Role of O_2

During the optimization of the reaction conditions, it was observed that the reaction gave a much higher yield under aerobic conditions. Various experimental[107–112] and theoretical studies[110,111] have shown that atmospheric oxygen (O_2) can oxidize Cu(I) species to Cu(II). In the current reaction, O_2 could facilitate the regeneration of the catalytic species by oxidizing the copper(I) complex (**Int1-M2**) to copper(II), which could undergo redox reactions with tetramethoxysilane to yield the catalytic species (Scheme 2). The calculated Gibbs free energies of the different steps involved in the oxidation of Cu(I) to Cu(II) are described in Scheme 7. In step (I), the iodide ligand of **Int1-M2** could be replaced by an acetate ligand to yield complex **9**, which could coordinate with an O_2 molecule to provide the O_2-coordinated complex **9**-O_2. The reaction of the Cs^+ ion with complex **9**-O_2 could generate Cu(II) complex **6** together with the formation of CsO_2. The calculated Gibbs free energies for the replacement of the iodide ligand with acetate, coordination of O_2 with complex **9** and formation of complex **6** are −5.0, −1.3 and +13.5 kcal mol^{-1}, respectively. Further reactions of

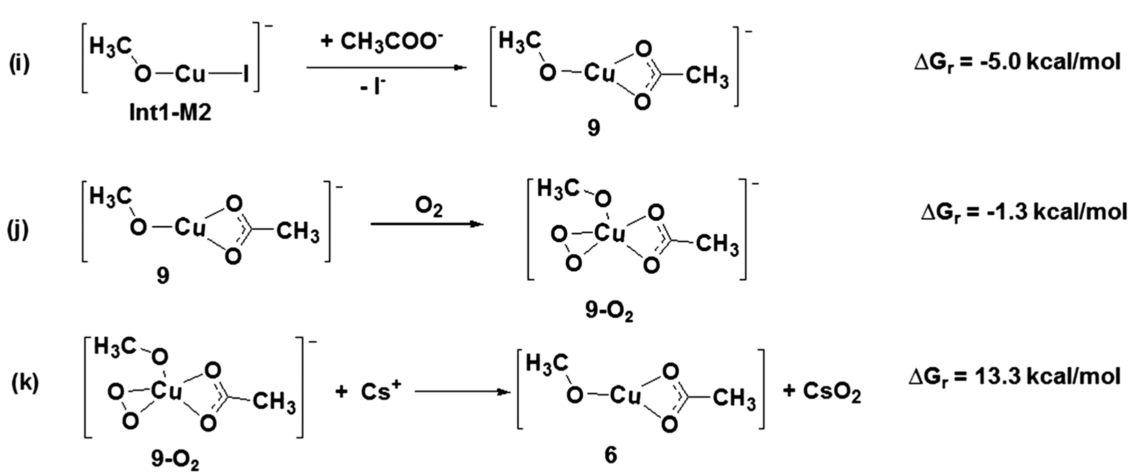

Scheme 7 Calculated Gibbs free energies for the aerobic oxidation of Cu(I) to Cu(II).

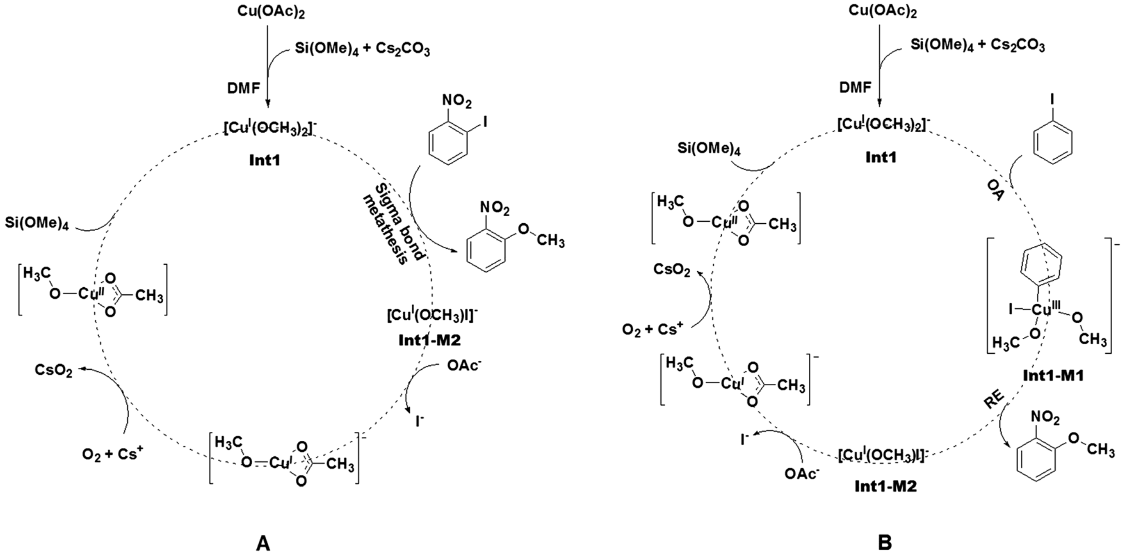

Fig. 6 Catalytic cycle **A** representing the etherification of 2-nitroiodobenzene by the σ-bond metathesis mechanism and catalytic cycle **B** representing the etherification of iodobenzene by the oxidative addition/reductive elimination mechanism.

complex **6** to generate catalytic species (**Int1**) are described in Scheme 2.

5. Catalytic cycle

The catalytic cycle for the reaction is given in Fig. 6. In catalytic cycle **A**, copper acetate reacts with tetramethoxysilane to generate the Cu(I) complex **Int1**. The σ-bond metathesis reaction of **Int1** and 2-nitroiodobenzene yields 1-methoxy-2-nitrobenzene and Cu(I) complex **Int1-M2**. The iodide ligand in **Int1-M2** is replaced with an acetate ligand to yield complex **9**. Atmospheric oxygen oxidizes the Cu(I) complex **9** to Cu(II) complex **6**, which on reaction with tetramethoxysilane yields the catalytic species **Int1**. The catalytic cycle **B** represents the etherification of iodobenzene through the oxidative addition/reductive elimination mechanism. The oxidative addition of iodobenzene to **Int1** affords the Cu(III) intermediate **Int1-M1**, which undergoes reductive elimination to yield methoxy benzene and Cu(I) intermediate **Int1-M2**. The replacement of the iodide ligand of **Int1-M2** with acetate, oxidation with O_2 and methoxylation with tetramethoxysilane regenerate the catalytic species **Int1**.

6. Conclusion

We developed an efficient route for the synthesis of diaryl and aryl alkyl ethers by the coupling reaction of aryl halides with alkoxy and aryloxy silanes in the presence of 20 mol% of copper acetate under oxidative conditions in DMF at 145 °C. The reaction setup was easy to perform and utilized aryl iodides, bromides and chlorides. A broad variety of functional groups was tolerated under the reaction conditions. A high degree of chemo-selectivity was also achieved in **2j**. DFT studies were carried out to study the mechanism of the reaction. Two plausible Cu(I) intermediates, **Int1** ($[Cu(OCH_3)_2]^-$) and **Int2** ($[Cu(OCH_3)(CH_3COO)]^-$), were selected for the mechanistic studies. Calculations were performed for the generation of catalytic species as well as for the oxidative addition/reductive elimination, σ-bond metathesis, single electron transfer and halogen atom transfer mechanisms for the C–O coupling step in the methoxylation of 2-nitroiodobenzene and iodobenzene. For the C–O coupling step, the σ-bond metathesis mechanism showed the lowest activation energy (16.0 kcal mol^{-1}) for the methoxylation of 2-nitroiodobenzene, whereas the oxidative addition/reductive elimination mechanism showed the lowest barrier (24.2 kcal mol^{-1}) for the methoxylation of iodobenzene. The calculated C–I bond dissociation energy of 2-nitroiodobenzene (45.4 kcal mol^{-1}) is significantly lower than the C–I bond dissociation energy of iodobenzene (53.9 kcal mol^{-1}) and is plausibly responsible for its facile C–O coupling reaction. The overall activation energy barrier for the generation of catalytic species (31.6 kcal mol^{-1}) through single electron transfer from tetramethoxysilane to copper acetate, formation of methoxy radicals and methoxylation of copper is the rate-determining reaction step. Thus, the calculated activation energy barrier is reasonable under the given experimental conditions (145 °C, 18 h).

Conflicts of interest

There are no conflicts to declare.

Acknowledgements

We are thankful to Higher Education Commission (HEC, PIN: IRSIP 22 Ps 29) Pakistan for financial support. We are also thankful to Shaanxi University of Technology for financial support to S. K. R. The DFT calculations were performed using the Shaanxi Key Laboratory of Catalysis, School of Chemical and Environmental Science, Shaanxi University of Technology, China.

References

1 S. Enthaler, Palladium-catalysed hydroxylation and alkoxylation, *Chem. Soc. Rev.*, 2011, **40**, 4912.

2 J. J. Li, D. S. Johnson, D. R. Sliskovic and B. D. Roth, *Contemporary drug synthesis*, John Wiley & Sons, 2004.

3 J. J. Li and D. S. Johnson, *Modern drug synthesis*, John Wiley & Sons, 2013.

4 H. G. Elias, *An introduction to polymer science*, VCH, 1997.

5 J. H. Montgomery, *Agrochemicals desk reference*, CRC Press, 1997.

6 J. P. Koilpillai, P. B. Kulkami, A. D. Dabe and M. A. Khan, Process for the preparation of esomeprazole magnesium dihydrate, EP2186807 A1, 2010.

7 A. Les, W. Pucko and W. Szelejewski, Optimization of the Reduction of a 5-Benzylidenethiazolidine-2,4-dione Derivative Supported by the Reaction Response Surface Analysis: Synthesis of Pioglitazone Hydrochloride, *Org. Process Res. Dev.*, 2004, **8**, 157.

8 S. P. Chavan, D. A. Khobragade, S. K. Kamat, L. Sivadasan, K. Balakrishnan, T. Ravindranathan, M. K. Gurjar and U. R. Kalkote, An efficient and green protocol for the preparation of cycloalkanols: a practical synthesis of venlafaxine, *Tetrahedron Lett.*, 2004, **45**, 7291.

9 M. B. Smith and J. March, *March's advanced organic chemistry: reactions, mechanisms, and structure*, John Wiley & Sons, 2007.

10 S. V. Ley and A. W. Thomas, Modern Synthetic Methods for Copper-Mediated C(aryl)[BOND]O, C(aryl)[BOND]N, and C(aryl)[BOND]S Bond Formation, *Angew. Chem., Int. Ed.*, 2003, **42**, 5400.

11 J. F. Hartwig, Carbon-heteroatom bond formation catalysed by organometallic complexes, *Nature*, 2008, **455**, 314.

12 J. F. Hartwig, Transition Metal Catalyzed Synthesis of Arylamines and Aryl Ethers from Aryl Halides and Triflates: Scope and Mechanism, *Angew. Chem., Int. Ed.*, 1998, **37**, 2046.

13 F. Monnier and M. Taillefer, Catalytic CC, CN, and CO Ullmann-Type Coupling Reactions, *Angew. Chem., Int. Ed.*, 2009, **48**, 6954.

14 K. E. Torraca, X. Huang, C. A. Parrish and S. L. Buchwald, An Efficient Intermolecular Palladium-Catalyzed Synthesis of Aryl Ethers, *J. Am. Chem. Soc.*, 2001, **123**, 10770.

15 S. Gowrisankar, A. G. Sergeev, P. Anbarasan, A. Spannenberg, H. Neumann and M. Beller, A General and Efficient Catalyst for Palladium-Catalyzed C–O Coupling Reactions of Aryl Halides with Primary Alcohols, *J. Am. Chem. Soc.*, 2010, **132**, 11592.

16 S. Gowrisankar, H. Neumann and M. Beller, A Convenient and Practical Synthesis of Anisoles and Deuterated Anisoles by Palladium-Catalyzed Coupling Reactions of Aryl Bromides and Chlorides, *Chem. – Eur. J.*, 2012, **18**, 2498.

17 Q. Zhang, D. Wang, X. Wang and K. Ding, (2-Pyridyl)-acetone-Promoted Cu-Catalyzed O-Arylation of Phenols with Aryl Iodides, Bromides, and Chlorides, *J. Org. Chem.*, 2009, **74**, 7187.

18 R. Zhang, J. Liu, S. Wang, J. Niu, C. Xia and W. Sun, Magnetic CuFe$_2$O$_4$ Nanoparticles as an Efficient Catalyst for CO Cross Coupling of Phenols with Aryl Halides, *ChemCatChem*, 2011, **3**, 146.

19 A. B. Naidu, E. Jaseer and G. Sekar, General, Mild, and Intermolecular Ullmann-Type Synthesis of Diaryl and Alkyl Aryl Ethers Catalyzed by Diol-Copper(I) Complex, *J. Org. Chem.*, 2009, **74**, 3675.

20 J. F. Marcoux, S. Doye and S. L. Buchwald, A General Copper-Catalyzed Synthesis of Diaryl Ethers, *J. Am. Chem. Soc.*, 1997, **119**, 10539–10540.

21 S. L. Buchwald and C. Bolm, On the Role of Metal Contaminants in Catalyses with FeCl$_3$, *Angew. Chem., Int. Ed.*, 2009, **48**, 5586–5587.

22 P. F. Larsson, A. Correa, M. Carril, P. O. Norrby and C. Bolm, Copper-Catalyzed Cross-Couplings with Part-per-Million Catalyst Loadings, *Angew. Chem., Int. Ed.*, 2009, **48**, 5691–5693.

23 O. Bistri, A. Correa and C. Bolm, Iron-Catalyzed C–O Cross-Couplings of Phenols with Aryl Iodides, *Angew. Chem., Int. Ed.*, 2008, **47**, 586–588.

24 D. Saberi, M. Sheykhan, K. Niknam and A. Heydari, Preparation of carbon nanotube-supported a-Fe$_2$O$_3$@CuO nanocomposite: a highly efficient and magnetically separable catalyst in cross-coupling of aryl halides with phenols, *Catal. Sci. Technol.*, 2013, **3**, 2025–2031.

25 P. S. Herradura, K. A. Pendola and R. K. Guy, Copper-Mediated Cross-Coupling of Aryl Boronic Acids and Alkyl Thiols, *Org. Lett.*, 2000, **2**, 2019.

26 C. Savarin, J. Srogl, L. S. Liebeskind and A. Mild, Nonbasic Synthesis of Thioethers. The Copper-Catalyzed Coupling of Boronic Acids with N-Thio(alkyl, aryl, heteroaryl)imides, *Org. Lett.*, 2002, **4**, 4309.

27 J. Simon, S. Salzbrunn, G. Surya Prakash, N. A. Petasis and G. A. Olah, Regioselective Conversion of Arylboronic Acids to Phenols and Subsequent Coupling to Symmetrical Diaryl Ethers, *J. Org. Chem.*, 2001, **66**, 633.

28 P. Y. Lam, C. G. Clark, S. Saubern, J. Adams, M. P. Winters, D. M. Chan and A. Combs, New Aryl/Heteroaryl C-N Bond Cross-coupling Reactions via Arylboronic Acid/Cupric Acetate Arylation, *Tetrahedron Lett.*, 1998, **39**, 2941.

29 K. S. Rao and T.-S. Wu, Chan–Lam coupling reactions: synthesis of heterocycles, *Tetrahedron*, 2012, **68**, 7735.

30 S. Bhadra, W. I. Dzik and L. J. Goossen, Decarboxylative Etherification of Aromatic Carboxylic Acids, *J. Am. Chem. Soc.*, 2012, **134**, 9938.

31 G. L. Witucki, A Silane Primer: Chemistry and Applications of AIkoxy Silanes, *J. Coat. Technol.*, 1993, **65**, 57.

32 E. R. Strieter, D. G. Blackmond and S. L. Buchwald, The role of chelating diamine ligands in the Goldberg reaction: a kinetic study on the copper-catalyzed amidation of aryl iodides, *J. Am. Chem. Soc.*, 2005, **127**, 4120–4121.

33 E. R. Strieter, B. Bhayana and S. L. Buchwald, Mechanistic studies on the copper-catalyzed N-arylation of amides, *J. Am. Chem. Soc.*, 2009, **131**, 78–88.

34 G. Franc, Q. Cacciuttolo, G. Lefèvre, C. Adamo, I. Ciofini and A. Jutand, Mechanistic Insights into C–N Coupling Catalyzed by 1,3-Diketonate-Ligated Copper: Unprecedented Activation of Aryl Iodide, *ChemCatChem*, 2011, **3**, 305–309.

35 G. Lefèvre, G. Franc, A. Tlili, C. Adamo, M. Taillefer, I. Ciofini and A. Jutand, Contribution to the Mechanism of Copper-Catalyzed C–N and C–O Bond Formation, *Organometallics*, 2012, **31**, 7694–7707.

36 K. K. Gurjar and R. K. Sharma, Mechanistic Studies of Ullmann Type C–N Coupling Reactions: Carbonate Ligated Cu(III) Intermediate, *ChemCatChem*, 2017, **9**, 862–869.

37 G. Lefèvre, A. Tlili, M. Taillefer, C. Adamo, I. Ciofini and A. Jutand, Discriminating role of bases in diketonate copper(I)-catalyzed C–O couplings: phenol versus diarylether, *Dalton Trans.*, 2013, **42**, 5348–5354.

38 G. O. Jones, P. Liu, K. N. Houk and S. L. Buchwald, Computational Explorations of Mechanisms and Ligand-Directed Selectivities of Copper-Catalyzed Ullmann-Type Reactions, *J. Am. Chem. Soc.*, 2010, **132**, 6205–6213.

39 S. Zhang and Y. Ding, Theoretical study on mechanism of copper(I)-catalyzed cross-coupling between aryl halides and alkylamines, *Organometallics*, 2011, **30**, 633–641.

40 H.-Z. Yu, Y.-Y. Jiang, Y. Fu and L. Liu, Alternative Mechanistic Explanation for Ligand-Dependent Selectivities in Copper-Catalyzed *N*- and *O*-Arylation Reactions, *J. Am. Chem. Soc.*, 2010, **132**, 18078–18091.

41 S. L. Zhang, L. Liu, Y. Fu and Q.-X. Guo, Theoretical Study on Copper(I)-Catalyzed Cross-Coupling between Aryl Halides and Amides, *Organometallics*, 2007, **26**, 4546–4554.

42 K. Ahmad, B. A. Khan, B. Akram, J. Khan, R. Mahmood and S. K. Roy, Theoretical investigations on copper catalyzed C-N cross-coupling reaction between aryl chlorides and amines, *Comput. Theor. Chem.*, 2018, **1134**, 1–7.

43 T. Chen, M. Yan, C. Zheng, J. Yuan, S. Xu, R. Chen and W. Huang, A Theoretical Insight into the Mechanism of Cu(I) Catalyzed C–N Coupling between Aryl Halides and Aqueous Ammonia, *Chin. J. Chem.*, 2015, **33**, 961–966.

44 H. Guo and Y. Xue, Theoretical Study on CuI-catalyzed Ligand-free N-arylation of Imidazole with Bromobenzene, *J. Theor. Comput. Chem.*, 2012, **11**, 1135–1148.

45 K. Ahmad, C.-R. Chang and J. Li, Theoretical studies on copper-catalyzed arylation of nitrogen heterocycles from benzenediazonium acetate under ligand-free conditions, *J. Organomet. Chem.*, 2018, **864**, 50–57.

46 C. R. David, Recent advances in silyl protection of alcohols, *Synth. Commun.*, 2013, **43**, 2265–2279.

47 M. N. Ahmed, A novel route to aromatic ethers and synthesis of biologically active heterocyclic esters/thioether, PhD thesis, University of Azad Jammu and Kashmir, Muzaffarabad, Pakistan, 2015, pp. 16–17.

48 A. E. King, T. C. Brunold and S. S. Stahl, Mechanistic Study of Copper-Catalyzed Aerobic Oxidative Coupling of Arylboronic Esters and Methanol: Insights into an Organometallic Oxidase Reaction, *J. Am. Chem. Soc.*, 2009, **131**, 5044.

49 M. J. Frisch, *et al.*, *Gaussian 09, Revision D.01*, Gaussian, Inc., Wallingford CT, 2009.

50 A. D. Becke, Density-functional thermochemistry. III. The role of exact exchange, *J. Chem. Phys.*, 1993, **98**, 5648.

51 C. Lee, W. Yang and R. G. Parr, Development of the Colle-Salvetti correlation-energy formula into a functional of the electron density, *Phys. Rev. B: Condens. Matter Mater. Phys.*, 1988, **37**, 785.

52 P. J. Stephens, F. J. Devlin, C. F. Chabalowski and M. J. Frisch, Ab Initio Calculation of Vibrational Absorption and Circular Dichroism Spectra Using Density Functional Force Fields, *J. Phys. Chem.*, 1994, **98**, 11623.

53 P. J. Hay and W. R. Wadt, *Ab Initio* effective core potentials for molecular calculations. Potentials for the transition metal atoms Sc to Hg, *J. Chem. Phys.*, 1985, **82**, 270–283.

54 H. B. Schlegel, Optimization of equilibrium geometries and transition structures, *J. Comput. Chem.*, 1982, **3**, 214–218.

55 M. Cossi, N. Rega, G. Scalmani and V. Barone, Energies, structures, and electronic properties of molecules in solution with the C-PCM solvation mode, *J. Comput. Chem.*, 2003, **24**, 669–681.

56 V. Barone and M. Cossi, Quantum Calculation of Molecular Energies and Energy Gradients in Solution by a Conductor Solvent Model, *J. Phys. Chem. A*, 1998, **102**, 1995–2001.

57 J. Andzelm, C. Kölmel and A. Klamt, Incorporation of solvent effects into density functional calculations of molecular energies and geometries, *J. Chem. Phys.*, 1995, **103**, 9312–9320.

58 F. Ullmann, Ueber Synthesen in der Biphenylreihe, *Chem. Ber.*, 1901, **34**, 2174–2185.

59 F. Ullmann, Ueber eine neue Bildungsweise von Diphenylaminderivaten, *Chem. Ber.*, 1903, **36**, 2382–2384.

60 F. Ullmann and P. Sponagel, Ueber die Phenylirung von Phenolen, *Chem. Ber.*, 1905, **38**, 2211–2212.

61 I. Goldberg, Ueber Phenylirungen bei Gegenwart von Kupfer als Katalysator, *Chem. Ber.*, 1906, **39**, 1691–1692.

62 Q. Shen, S. Shekhar, J. P. Stambuli and J. F. Hartwig, Highly Reactive, General, and Long-Lived Catalysts for Coupling Heteroaryl and Aryl Chlorides with Primary Nitrogen Nucleophiles, *Angew. Chem., Int. Ed.*, 2005, **44**, 1371–1375.

63 X. Huang, K. W. Anderson, D. Zim, L. Jiang, A. Klapars and S. L. Buchwald, Expanding Pd-Catalyzed C–N Bond-Forming Processes: The First Amidation of Aryl Sulfonates, Aqueous Amination, and Complementarity with Cu-Catalyzed Reactions, *J. Am. Chem. Soc.*, 2003, **125**, 6653–6655.

64 A. Kiyomori, J.-F. Marcoux and S. L. Buchwald, An efficient copper-catalyzed coupling of aryl halides with imidazoles, *Tetrahedron Lett.*, 1999, **40**, 2657–2660.

65 H. B. Goodbrand and N.-X. Hu, Ligand-Accelerated Catalysis of the Ullmann Condensation: Application to Hole Conducting Triarylamines, *J. Org. Chem.*, 1999, **64**, 670–674.

66 R. K. Gujadhur, C. G. Bates and D. Venkataraman, Formation of aryl-nitrogen, aryl-oxygen, and aryl-carbon bonds using well-defined copper(I)-based catalysts, *Org. Lett.*, 2001, **3**, 4315–4317.

67 F. Y. Kwong, A. Klapars and S. L. Buchwald, Copper-Catalyzed Coupling of Alkylamines and Aryl Iodides: An Efficient System Even in an Air Atmosphere, *Org. Lett.*, 2002, **4**, 581–584.

68 D. Ma, Q. Cai and H. Zhang, Mild Method for Ullmann Coupling Reaction of Amines and Aryl Halides, *Org. Lett.*, 2003, **5**, 2453–2455.

69 F. Y. Kwong and S. L. Buchwald, Mild and efficient copper-catalyzed amination of aryl bromides with primary alkylamines, *Org. Lett.*, 2003, **5**, 793–796.

70 J. C. Antilla, J. M. Baskin, T. E. Barder and S. L. Buchwald, Copper-Diamine-Catalyzed *N*-Arylation of Pyrroles, Pyrazoles, Indazoles, Imidazoles, and Triazoles, *J. Org. Chem.*, 2004, **69**, 5578–5587.

71 J. Zanon, A. Klapars and S. L. Buchwald, Copper-Catalyzed Domino Halide Exchange-Cyanation of Aryl Bromides, *J. Am. Chem. Soc.*, 2003, **125**, 2890–2891.

72 L. Jiang, G. E. Job, A. Klapars and S. L. Buchwald, Copper-Catalyzed Coupling of Amides and Carbamates with Vinyl Halides, *Org. Lett.*, 2003, **5**, 3667–3669.

73 A. Klapars and S. L. Buchwald, Copper-Catalyzed Halogen Exchange in Aryl Halides: An Aromatic Finkelstein Reaction, *J. Am. Chem. Soc.*, 2002, **124**, 14844–14845.

74 J. C. Antilla, A. Klapars and S. L. Buchwald, The copper-catalyzed *N*-arylation of indoles, *J. Am. Chem. Soc.*, 2002, **124**, 11684–11688.

75 A. Klapars, X. Huang and S. L. Buchwald, A general and efficient copper catalyst for the amidation of aryl halides, *J. Am. Chem. Soc.*, 2002, **124**, 7421–7428.

76 A. Klapars, J. C. Antilla, X. Huang and S. L. Buchwald, A General and Efficient Copper Catalyst for the Amidation of Aryl Halides and the *N*-Arylation of Nitrogen Heterocycles, *J. Am. Chem. Soc.*, 2001, **123**, 7727–7729.

77 P. W. Weston and H. Adkins, Catalysis with copper in the Ullmann reaction, *J. Am. Chem. Soc.*, 1928, **50**, 859–866.

78 E. Sperotto, G. P. M. van Klink, G. van Koten and J. G. de Vries, The mechanism of the modified Ullmann reaction, *Dalton Trans.*, 2010, **39**, 10338–10351.

79 Z. Tye, J. W. Weng, A. M. Johns, A. C. D. Incarvito and J. F. Hartwig, Copper complexes of anionic nitrogen ligands in the amidation and imidation of aryl halides, *J. Am. Chem. Soc.*, 2008, **130**, 9971–9983.

80 R. Giri and L. F. Hartwig, Cu(I)–Amido Complexes in the Ullmann Reaction: Reactions of Cu(I)–Amido Complexes with Iodoarenes with and without Autocatalysis by CuI, *J. Am. Chem. Soc.*, 2010, **132**, 15860–15863.

81 J. W. Tye, Z. Weng and R. Giri, Copper(I) phenoxide complexes in the etherification of aryl halides, J. F. Hartwig, *Angew. Chem., Int. Ed.*, 2010, **49**, 2185–2189.

82 G. Lefèvre, G. Franc, C. Adamo, A. Jutand and I. Ciofini, Influence of the Formation of the Halogen Bond ArX···N on the Mechanism of Diketonate Ligated Copper-Catalyzed Amination of Aromatic Halides, *Organometallics*, 2012, **31**, 914–920.

83 M. Mansour, R. Giacovazzi, A. Ouali, M. Taillefer and A. Jutand, Activation of aryl halides by Cu(0)/1,10-phenanthroline: Cu(0) as precursor of Cu(I) catalyst in cross-coupling reactions, *Chem. Commun.*, 2008, 6051–6053.

84 G. Franc and A. Jutand, On the origin of copper(I) catalysts from copper(II) precursors in C–N and C–O cross-couplings, *Dalton Trans.*, 2010, **39**, 7873–7875.

85 H. Weingarten, Mechanism of the Ullmann Condensation, *J. Org. Chem.*, 1964, **29**, 3624–3626.

86 A. J. Paine, Mechanisms and models for copper mediated nucleophilic aromatic substitution. 2. Single catalytic species from three different oxidation states of copper in an Ullmann synthesis of triarylamines, *J. Am. Chem. Soc.*, 1987, **109**, 1496–1502.

87 H. L. Aalten, G. van Koten, D. M. Grove, T. Kuilman, O. G. Piekstra, L. A. Hulshof and R. A. Sheldon, The copper catalysed reaction of sodium methoxide with aryl bromides. A mechanistic study leading to a facile synthesis of anisole derivatives, *Tetrahedron*, 1989, **45**, 5565–5578.

88 R. Resnik, T. Cohen and Q. Fernando, The phenol oxidation of a ligand by copper(II), *J. Am. Chem. Soc.*, 1961, **83**, 3344–3345.

89 S. Zhu, N. Niljianskul and S. L. Buchwald, Enantio- and Regioselective CuH-Catalyzed Hydroamination of Alkenes, *J. Am. Chem. Soc.*, 2013, **135**, 15746–15749.

90 S. Zhu and S. L. Buchwald, Enantioselective CuH-Catalyzed Anti-Markovnikov Hydroamination of 1,1-Disubstituted Alkenes, *J. Am. Chem. Soc.*, 2014, **136**, 15913–15916.

91 N. Niljianskul, S. Zhu and S. L. Buchwald, Enantioselective Synthesis of α-Aminosilanes by Copper-Catalyzed Hydroamination of Vinylsilanes, *Angew. Chem., Int. Ed.*, 2015, **54**, 1638–1641.

92 E. Ascic and S. L. Buchwald, Highly Diastereo- and Enantioselective CuH-Catalyzed Synthesis of 2,3-Disubstituted Indolines, *J. Am. Chem. Soc.*, 2015, **137**, 4666–4669.

93 J. Selvakumar, G. S. Grandhi, H. Sahoo and M. Baidya, Copper-mediated etherification of arenes with alkoxysilanes directed by an (2-aminophenyl)pyrazole group, *RSC Adv.*, 2016, **6**, 79361–79365.

94 R. A. Marcus, On the Theory of Oxidation-Reduction Reactions Involving Electron Transfer. I, *J. Chem. Phys.*, 1956, **24**, 966–978.

95 R. A. Marcus, Electrostatic Free Energy and Other Properties of States Having Nonequilibrium Polarization. I, *J. Chem. Phys.*, 1956, **24**, 979–989.

96 R. A. Marcus, On the Theory of Oxidation-Reduction Reactions Involving Electron Transfer. III. Applications to Data on the Rates of Organic Redox Reactions, *J. Chem. Phys.*, 1957, **26**, 872–877.

97 N. S. Hush, Adiabatic Rate Processes at Electrodes. I. Energy-Charge Relationships, *J. Chem. Phys.*, 1958, **28**, 962–972.

98 R. A. Marcus, On the Theory of Electrochemical and Chemical Electron Transfer Processes, *Can. J. Chem.*, 1959, **37**, 155–163.

99 N. S. Hush, Adiabatic theory of outer sphere electron-transfer reactions in solution, *Trans. Faraday Soc.*, 1961, **57**, 557–580.

100 R. A. Marcus, On the Theory of Electron-Transfer Reactions. VI. Unified Treatment of Homogeneous and Electrode Reactions, *J. Chem. Phys.*, 1965, **43**, 679–701.

101 R. A. Marcus and N. Sutin, Electron Transfers in Chemistry and Biology, *Biochem. Biophys. Acta*, 1985, **811**, 265–322.

102 C. Chuit, R. J. P. Corriu, C. Reye and J. C. Young, Reactivity of Penta- and Hexacoordinate Silicon Compounds and

Their Role as Reaction Intermediates, *Chem. Rev.*, 1993, **93**, 1371–1448.

103 J.-M. Savéant, A simple model for the kinetics of dissociative electron transfer in polar solvents. Application to the homogeneous and heterogeneous reduction of alkyl halides, *J. Am. Chem. Soc.*, 1987, **109**, 6788–6795.

104 J.-M. Savéant, Dissociative electron transfer. New tests of the theory in the electrochemical and homogeneous reduction of alkyl halides, *J. Am. Chem. Soc.*, 1992, **114**, 10595–10602.

105 J.-M. Savéant, Electron transfer, bond breaking, and bond formation, *Acc. Chem. Res.*, 1993, **26**, 455–461.

106 K. Ahmad, C.-R. Chang and J. Li, Mechanistic investigations of Co(II)-Catalyzed C-N coupling reactions, *J. Organomet. Chem.*, 2018, **868**, 144–153.

107 P. Keil, D. Lützenkirchen-Hecht and R. Frahm, Investigation of Room Temperature Oxidation of Cu in Air by Yoneda-XAFS, *AIP Conf. Proc.*, 2007, **882**, 490.

108 E. Apen, B. R. Rogers and J. A. Sellers, X-ray photoelectron spectroscopy characterization of the oxidation of electroplated and sputter deposited copper surfaces, *J. Vac. Sci. Technol., A*, 1998, **16**, 1227.

109 R. D. Gray, The Kinetics of Oxidation of Copper(I) by Molecular Oxygen in Perchloric Acid-Acetonitrile Solutions, *J. Am. Chem. Soc.*, 1969, **91**, 56.

110 C. H. Kjaergaard, M. F. Qayyum, S. D. Wong, F. Xu, G. R. Hemsworth, D. J. Walton, N. A. Young, G. J. Davies, P. H. Walton, K. S. Johansen, K. O. Hodgson, B. Hedman and E. I. Solomon, Spectroscopic and computational insight into the activation of O^2 by the mononuclear Cu center in polysaccharide monooxygenases, *Proc. Natl. Acad. Sci. U. S. A.*, 2014, **111**, 8797.

111 B. V. Popp, J. E. Wendlandt, C. R. Landis and S. S. Stahl, Reaction of Molecular Oxygen with an NHC-Coordinated Pd^0 Complex: Computational Insights and Experimental Implications, *Angew. Chem., Int. Ed.*, 2007, **46**, 601–604.

112 A. N. Campbell and S. S. Stahl, Overcoming the ''Oxidant Problem'': Strategies to Use O_2 as the Oxidant in Organometallic C–H Oxidation Reactions Catalyzed by Pd (and Cu), *Acc. Chem. Res.*, 2012, **45**, 851–863.